Journal of Magnetism and Magnetic Materials 427 (2017) 195–199

Contents lists available at ScienceDirect

Journal of Magnetism and Magnetic Materials

journal homepage: www.elsevier.com/locate/jmmm

Improving heat generation of magnetic nanoparticles by pre-orientation of particles in a static three tesla magnetic field

Mathias M. Beck[a,*], Christian Lammel[a], Bernhard Gleich[b]

[a] Institute for Machine Tools and Industrial Management, Technical University of Munich, Boltzmannstr. 15, 85748 Garching, Germany
[b] Institute of Medical Engineering, Technical University of Munich, Boltzmannstr. 11, 85748 Garching, Germany

ARTICLE INFO

Keywords:
Magnetic nanoparticle
Specific Absorption Rate (SAR)
Heating
Alignment
Orientation

ABSTRACT

Inductive heating of electrically insulating materials like fiberglass reinforced thermoplastics (FRTP) without susceptors is not possible. However, due to their low thermal conductivity a volumetric heat generation method is advisable to reach short heating times to melt this material for reshaping. This can be done with magnetic nanoparticles as susceptors within the thermoplastic of the FRTP using Néel relaxation. During the heating process the particle's magnetic moment rotates with the field while the particle itself is fixed within the thermoplastic. Therefore the heat dissipation of each particle depends on its orientation within the field. To achieve the maximum heat generation of the particles we pre-oriented the particles within a plastic at the best angle to the applied AC field for induction. To do this, five mass percent nanoparticles were dispersed in an epoxy resin, which was then hardened at room temperature in a static three Tesla magnetic field. After its solidification the heating behavior of the sample was compared to a reference sample, which was hardened without a field. The oriented particles showed an increased heating rate when oriented parallel to the applied AC field. The absorption rate was 3.3 times as high as the undirected reference sample. When the alternating electromagnetic field was perpendicular to the oriented particles, the specific absorption rate was similar to that of the reference sample. We compare this result with theory and with calculations from literature, and conduct a numerical simulation.

1. Introduction

Due to the increased use of lightweight materials in the area of mechanical engineering, especially aeronautical and automotive engineering, there is also an increased need of fast production methods for these materials [1]. Within this field reinforced thermoplastics, for example using fiberglass, have strong potential due to their reshapeability and better recyclability compared to thermoset components [2]. These thermoplastic materials are generally hot pressed during manufacturing, which is a fast process only for flat samples due to their low thermal conductivity that results in only small possible heat input through the surface of the components [3]. In order to form and reshape thermoplastic composites the duration and energy consumption of this process is a problem to address. Due to the high thermal conduction, thicker samples in particular can only be heated slowly as the temperature on the surface is limited by the degradation temperature of the thermoplastic. This makes it difficult to achieve a relevant production speed in commercial applications. Volumetric heating using magnetic nanoparticles as susceptor for inductive energy transfer is one possible way to overcome this constraint. Induction heating using nanoscale particles allows energy transfer into and volumetric heat generation within the particles. This avoids the heat transfer limit via the surface of the composite and therefore has a potential for increasing the production speed.

In general, there are two possible mechanisms regarding nanoparticle heating: Brown relaxation heating occurs due to frictional losses while the particle rotates in a fluid, Néel relaxation heating by rotation and fluctuation of the magnetic moment using the different energy levels due to the magnetic anisotropy of the particle [4]. Many studies are being conducted in the medical field, mainly with respect to Brown relaxation using ferrofluids [5–9], but only few studies have been conducted in the field of mechanical engineering regarding nanoparticle heating within solid matrices. Tay et al. [10] presented a proof of concept for rapid curing of bonds using inductively heated nanoparticles, and tested the resulting bonds for the reduction of strength due to the particles. He showed that nanoparticles are suitable for the demands of mechanical engineering. Temperature profiles concerning the reaction of resins and the energy absorption of ferritic particles were modeled by Ye et al. [11]. Miller et al. [12] heated epoxy resin in about 70 s over 100 °C using FeCo particles, a frequency of 26 kHz and

* Corresponding author.
E-mail address: Mathias.Beck@tum.de (M.M. Beck).

http://dx.doi.org/10.1016/j.jmmm.2016.11.005
Received 24 June 2016; Received in revised form 19 October 2016; Accepted 1 November 2016
Available online 03 November 2016

an electromagnetic field strength of 20.0 kA/m. These are parameters that are realistic for larger scale manufacturing, but still the heating rate is not high enough with respect to the production cycle times in automotive engineering of 60 s and the demanded temperature increase of about 250 °C up to the melting temperature of generally used thermoplastics such as polyamide. It follows that there is a need for large energy absorption of particles that are low in price and available in large amounts, a requirement which is hard to fulfill.

To achieve the full energy absorption/heat generation of particles that are dispersed in a solid material, we oriented magnetic nanoparticles parallel to the magnetic AC field. Since the energy absorption in such a system is dependent on the orientation of the particle with respect to the applied field, we have shown that with the help of this alignment the heat generation can be increased significantly.

2. Theory

The heating mechanism for an inductively heated particle is dominated by the relaxation mechanism that has the shorter time constant [13]. For Néel (τ_N) and Brown relaxation (τ_B), these relaxation times are given by:

$$\tau_N = \tau_0 exp\frac{KV_M}{k_B T} \quad (1)$$

$$\tau_B = \frac{3\eta V_H}{k_B T} \quad (2)$$

Where $\tau_O=10^{-9}$ s, K is the anisotropy constant, V_M the volume of the particle, k_B the Boltzmann constant, T the temperature, η the viscosity and V_H the hydrodynamic particle volume. The effective relaxation time results to

$$\frac{1}{\tau}=\frac{1}{\tau_B}+\frac{1}{\tau_N} \quad (3)$$

As the viscosity of solid materials is very high, Néel relaxation dominates the heating mechanism of magnetic nanoparticles with an electromagnetic AC field when fixed in a solid plastic. There the particles cannot move and only their magnetization rotates with the field. In this case, the amount of energy absorption by the particle, which is proportional to the heat generation, depends on the angle φ between the particle's easy axis and the external magnetic AC field (Fig. 1). If this angle is zero – meaning the particle's easy axis is aligned with respect to the electromagnetic AC field – the amount of energy absorption is maximized [4]. The magnetic field and magnetization are aligned with respect to the easy axis. In the general case, without any external force acting on the particles, they have a statistically random orientation in space. The aim of this work is to orient the particles in space so as to increase the energy absorption.

The remanence and coercivity of a randomly oriented particle system are both approximately half of the value of the oriented case [5,14]. This leads to a four times higher theoretical energy absorption of the aligned particles (φ=0) in a Stoner-Wohlfarth-model [15]. Briefly this model describes the mechanism of magnetic hysteresis and can be used for magnetic nanoparticles.

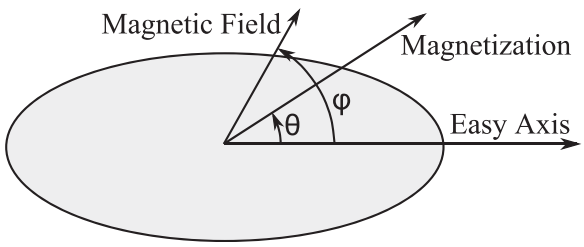

Fig. 1. Sketch of particle magnetization in magnetic field. If the external field is not aligned with the easy axis the magnetization of the particle rotates out of the energetic optimal axis. Therefore the maximal energy absorption cannot be reached.

The energy absorption in Néel relaxing systems is proportional to its hysteresis area [16]. A semi-analytical calculation, backed by numerical simulations, of hysteresis loops for the random oriented case is [4]

$$A(T)=4 \quad M_S\mu_0 H_K(1-\kappa^{0.5}) \quad (4)$$

and for the φ=0 case

$$A(T)=0.96 \quad M_S\mu_0 H_K(1-\kappa^{0.8}) \quad (5)$$

with the saturation magnetization M_S, the anisotropy field $\mu_O H_K$ and the factor κ defined as

$$\kappa = \frac{k_B T}{K_{eff} V}\ln\left(\frac{k_B T}{4 \quad \mu_0 H_{max} M_S V f \tau_0}\right) \quad (6)$$

with the Boltzmann constant k_B, the temperature T, the effective anisotropy K_{eff}, the volume V, the frequency factor of the Néel-Brown relaxation time τ_O, the frequency f and amplitude $\mu_O H_{max}$ of the electromagnetic AC field. When restricting the calculation to the hysteresis loops in the intermediate to high dissipation limit (κ~1, [17]) the influence of the exponents of κ disappears and the first factor of Eqs. 4 and 5 determines the different hysteresis areas. The hysteresis area of the aligned nanoparticles compared to the unaligned case is larger by the factor of 4/0.96=4.17. As the heat generation is proportional to the hysteresis area, it is expected to increase by the same factor when aligning the particles to the AC magnetic field.

3. Material and methods

3.1. Simulation

The simulation was conducted using the micro magnetic simulation package *NMAG-sim (University of Southampton, United Kingdom)*. 400 evenly distributed spherical particles with a core diameter size of 20 nm were simulated, which is the upper value of the particles' nominal single diameter used in the experiment given in the datasheet. To achieve an ideal result, the distance between the particles was increased until all interactions between the particles vanished at 160 nm. The Landau-Lifshitz-Gilbert damping parameter was set to 0.1 and the exchange coupling to 2.1e-11 J/m. Three different simulations were conducted differing in the orientation of the particle's easy axis with respect to the applied field – parallel, perpendicular and randomly oriented.

3.2. Particles

Uncoated iron(II, III) oxide (Fe_3O_4) particles were purchased from *IoLiTec (Ionic Liquids Technologies GmbH, Germany)*. According to the data provided these particles had a nominal average particle size of 15–20 nm and a purity of at least 99.5%. These spherical particles were delivered as a powder which was then prepared.

3.3. Dynamic Light Scattering (DLS)

36.5 mg particles were put in a fluid of 2 ml H_2O and 1 ml 10 mM HNO_3. This dispersion was vortexed for five minutes and dispersed by ultrasound for 6 h. The size of the particles was measured with a Zetasizer NanoZS (*Malvern Instruments GmbH, Germany*).

3.4. Sample Preparation

The epoxy resin-hardener-combination "SR 1720/ SD 7840" (*Sicomin Epoxy Systems, France)* was used as matrix for the samples. First the particle-powder was stirred into the resin. The mixture was mingled using ultrasound pulses for 60 min while being constantly cooled in a water quench (120 W at 30 kHz with a duty cycle of 25%

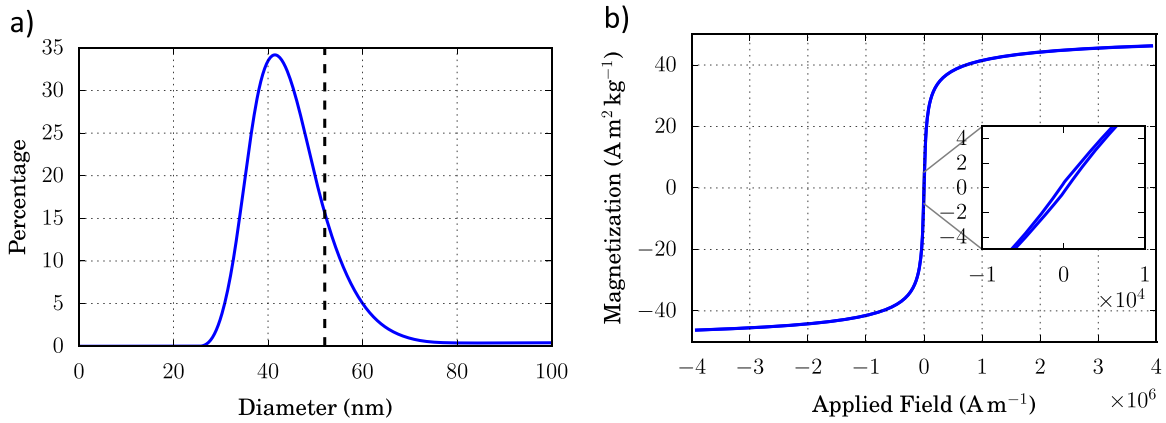

Fig. 2. Number weighted size of the particles measured with DLS (a) and magnetization curve (b). The particles have a mean agglomeration size of 52 nm (dashed line) and a close hysteresis loop.

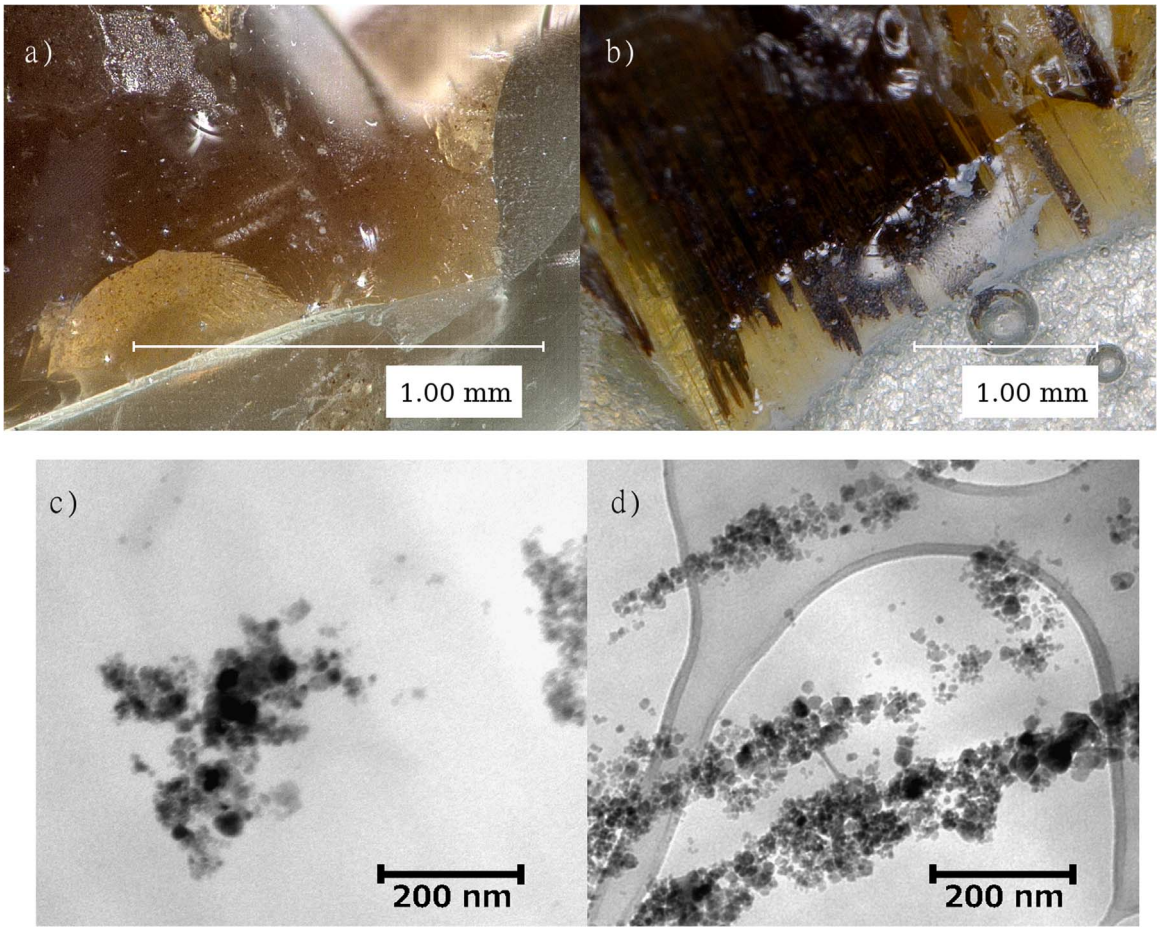

Fig. 3. Optical microscope picture of the unaligned (a) and aligned (b) sample and TEM micrographs from unaligned (c) and aligned (d) particles. The aligned particles form large needle like structures (b) which cannot be seen in the reference sample (a). While (c) show spherical agglomerates the agglomerates in (d) are elongated due to the external magnetic field during epoxy hardening.

using a ProteUS from *EM-Systeme GmbH, Germany*). Then the hardener was mixed into this dispersion using ultrasound for another three minutes. The particle content was five mass percent in total, the total specimen mass 15 g in a cylindrical shape with a diameter of 21 mm. A specimen of this mixture was put in a homogeneous static magnetic field of a magnetic resonance imaging system (3 T MRI, GE 750 MW) for 24 h. A reference sample was hardened in parallel under the same conditions without a magnetic field.

3.5. SAR measurement

The specific absorption rate (SAR, heat generation based on the pure particles) was calculated as $SAR=(m_s/\ m_p)c(\Delta T/t)$, with the masses m_s of the specimen and m_p of the particles, the heat capacity of sample c (1,68 J/kg K) and the specimen temperature increase during the AC field application ΔT which is applied for a time duration t. The measurement started 30 s after applying the field, with a measuring time of 90 s reaching maximum temperatures up to 95 °C. This method had a higher reproducibility than similar methods that

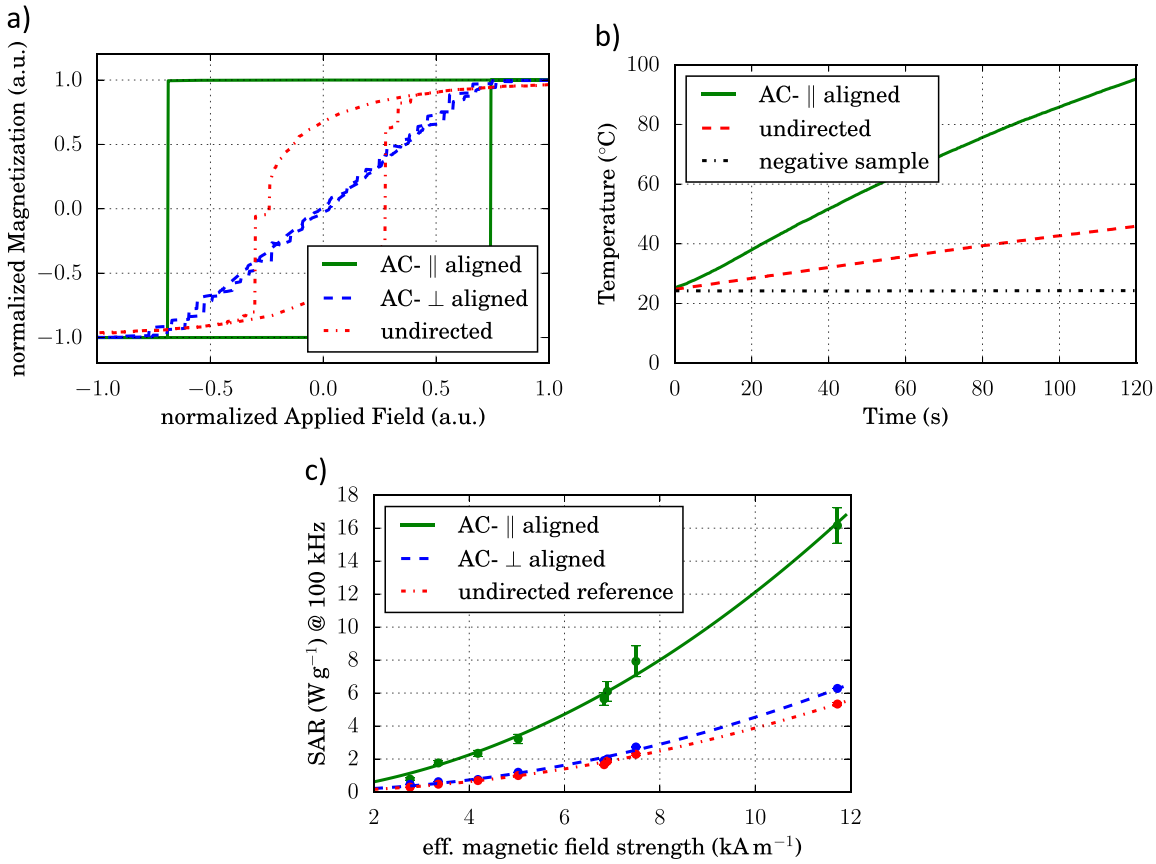

Fig. 4. Results of simulation (a) and SAR measurements raw data (b) and evaluated data (c) comparing aligned and unaligned particles. The raw data was investigated at different frequencies and field strengths (here 330 kHz and 6.9 kA/m) while the SAR was normalized to 100 kHz as described in Section 3.5.

rely on a shorter measurement time.

Measurement of the SAR was conducted using a "Magnetherm" system (*nanoTherics Ltd., United Kingdom)* in combination with a GaAs-sensor system (*opSens, France*) which was positioned in the middle of the specimen in a centric hole just the size of the sensor. The specimens were heated in a polystyrene insulation for two minutes. The MRI specimen was measured in different orientations of the particles' alignment to the electromagnetic AC-field, parallel and perpendicular.

The SAR of the particles used showed a linear frequency dependence in the applied frequency range of 109.8 kHz up to 985.9 kHz. This is a behavior well-documented in literature [5,18–20] which we use to normalize the SAR to the frequency. As the maximum possible electromagnetic field strength in the device used for the investigation of the SAR is limited and large field strength can only be reached at low frequencies, these low frequencies have to be used to investigate the behavior. Due to the mechanism of the heating device, however, high frequencies allow a finer adjustment of the field strength, which reduces possible errors that may occur due to inexact adjusted values. Thus there is an interest in the use of higher frequencies when investigating lower field strengths. As the results are easier to understand when they all refer to the same frequency and the SAR has the linear frequency dependence described above, in this work the SAR values are linearly normalized to 100 kHz. A normalization of the SAR regarding the frequency simplifies the comparison of the heating abilities between different publications.

3.6. Further analysis

Further analysis of the specimen described in Section 3.4 was conducted to provide an analysis of the particles for better reproducibility and comparability of the results. Magnetization measurements were conducted only on the reference sample using a magnetic properties measurement system (*Quantum Design, USA*) to provide the magnetization properties for classifying the SAR. A *CM-12 (Philips, Netherlands)* with a LaB6 emitter was used for TEM imaging in order to compare particle agglomeration and alignment in the samples. Sections of the samples were prepared using a diamond knife with a water filled boat and a microtome. The slices were directly retrieved from the blade's waterbed onto carbon-coated copper grids. The chosen thickness of 250 nm provided good permeability through the epoxy resin and did also show a considerable quantity of particles to determine a possible effect of field alignment.

4. Results and discussion

In the experiment the particles showed a number weighted size peak at 43 nm in DLS while the average size is 52 nm (see Fig. 2a). This means that there are many small but also very large agglomerates of particles.

The saturation magnetization of the random oriented particles in the epoxy is 46 Am^2/kg. The remanent magnetization is 0.38 Am^2/kg with a coercivity of 390 A/m. So the hysteresis area is very small (see Fig. 2b). This may be due to agglomeration, but could also be due to oxidation of the particles. Rümenapp et al. [21] showed that especially within the first 12 h after preparation there is a large change in magnetite content of uncoated particles, which is a reason for reduction of the hysteresis area.

Optical microscope pictures showed that needle-like structures have been formed in the oriented sample that could not be seen in the undirected reference sample (see Fig. 3a,b). The particles not only rotate within the epoxy but form large agglomerated structures. Large structures are known to change the magnetic properties of a nanoparticle system [22]. These structures can also be seen in the TEM pictures (Fig. 3c,d). The TEM pictures of the undirected reference sample show

two large spherical agglomerates and several smaller agglomerates and some individual particles. This is in accordance with the number weighted DLS result. An optical analysis of the sizes in the TEM was not conducted due to the large agglomerates and the small size of the snippet.

The result of the simulation can be seen in Fig. 4a. The simulation showed the hysteresis loop to have 4.01 times the area for the aligned compared to the random case. As described above, the SAR is proportional to the hysteresis area. Therefore it increases by the same factor. This factor is similar to the simulation backed analytical calculation where the result suggests a 4.17 times higher SAR. The perpendicularly oriented particles showed a close hysteresis with only a small hysteresis area, much smaller than in the undirected case with random orientation which results in a typical hysteresis shape.

The SAR depended on the angle between the applied electromagnetic AC field and the previously applied static field, as can be seen in Fig. 4b,c. At a field strength of 6.9 kA/m the aligned particles showed an SAR of 6.10 W/g at 100 kHz which is 3.3 times the heating rate of the undirected reference sample which showed 1.86 W/g. This is also the average increase over all measurements, resulting in 3.3/4.17=0.79 times the theoretical value of the theory section and 3.3/4.01=0.82 times the value of our simulation. This indicates that most particles could be aligned. The perpendicular measurement resulted in 2.00 W/g which is 1.075 times the heating rate of the undirected reference sample. Over all measurements this heating rate is slightly higher with a factor of 1.2 compared to the reference sample and standard deviation of 0.16. This is not in accordance with particle theory. A possible reason for this increase may be caused by the positioning of the sample or the sensor. Another possible reason is a change of the magnetic properties due to the built particle structures as described in the previous paragraph [22].

5. Conclusions

The heating rate could be increased by the factor of 3.3 with prior aligning of the particles parallel to the magnetic AC field. Therefore we could reach 0.79 times the maximum theoretically possible heating rate that was calculated in the theory section. We expect this behavior to be similar for different kinds of particles, that SAR can be increased significantly without changing the synthesis of the particles. This can improve the production of nanoparticle filled polymer composite materials. Targeted temperatures in commercial application for melting polyamide are around 250 °C. In the context of the present work, these temperatures were not expected to be reached. With increasing field strength and frequency to industrial scale it is possible to reach those temperatures within 10 s for small polymer sheets of less than 100 mm^2 (the field strength could not be measured, which is why the results are not published). However the efficiency is not high enough for heating larger specimens. A possible way to increase the heating rate is the coating of nanoparticles to prevent oxidation. Regarding the orientation of particles there is a need to show that this aligning can also be done with a smaller static field strength and can be implemented in the production of polymer fibers for composites.

Acknowledgment

The authors would like to thank Hinrich Grefe and Stefan Kreling of the *Institute of Joining and Welding* of the *Technische Universität Braunschweig* for sample preparation and TEM imaging. They would like to thank Christine Rümenapp and Alexander Joos of the *TUM Institute of Medical Engineering* for help with the experimental setup. They also thank Maximilian Schäfer from the *TUM Institute for Carbon Composites* for help with sample preparation. This research has been supported by the *German Federal Ministry of Education and Research* (project no.: 03×0147A-G).

References

[1] K. Friedrich, A.A. Almajid, Manufacturing aspects of advanced polymer composites for automotive applications, Appl. Compos. Mater. 20 (2013) 107–128. http://dx.doi.org/10.1007/s10443-012-9258-7.
[2] G. Koronis, A. Silva, M. Fontul, Green composites: a review of adequate materials for automotive applications, Compos. Part B: Eng. 44 (2013) 120–127. http://dx.doi.org/10.1016/j.compositesb.2012.07.004.
[3] M. Ho, H. Wang, J.-H. Lee, C.-K. Ho, K.-T. Lau, J. Leng, D. Hui, Critical factors on manufacturing processes of natural fibre composites, Compos. Part B: Eng. 8 (2012) 3549–3562. http://dx.doi.org/10.1016/j.compositesb.2011.10.001.
[4] J. Carrey, B. Mehdaoui, M. Respaud, Simple models for dynamic hysteresis loop calculations of magnetic single-domain nanoparticles: application to magnetic hyperthermia optimization, J. Appl. Phys. 109 (2011) 83921. http://dx.doi.org/10.1063/1.3551582.
[5] R.Hergt, W.Andra, C.D'Ambly, Physical limits of hyperthermia using magnetite fine particles, Magn. IEEE .... 343745–3754. ⟨http://ieeexplore.ieee.org/xpls/abs_all.jsp?Arnumber=718537⟩ (accessed 18.09.13), 1998.
[6] M. Suto, Y. Hirota, H. Mamiya, A. Fujita, R. Kasuya, K. Tohji, B. Jeyadevan, Heat dissipation mechanism of magnetite nanoparticles in magnetic fluid hyperthermia, J. Magn. Magn. Mater. 321 (2009) 1493–1496. http://dx.doi.org/10.1016/j.jmmm.2009.02.070.
[7] I. Nándori, J. Rácz, Magnetic particle hyperthermia: power losses under circularly polarized field in anisotropic nanoparticles, Phys. Rev. E 86 (2012) 61404. http://dx.doi.org/10.1103/PhysRevE.86.061404.
[8] G.T. Landi, Simple models for the heating curve in magnetic hyperthermia experiments, J. Magn. Magn. Mater. 326 (2013) 14–21. http://dx.doi.org/10.1016/j.jmmm.2012.08.034.
[9] A.E. Deatsch, B. a. Evans, Heating efficiency in magnetic nanoparticle hyperthermia, J. Magn. Magn. Mater. 354 (2014) 163–172. http://dx.doi.org/10.1016/j.jmmm.2013.11.006.
[10] T.E. Tay, B.K. Fink, S.H. McKnight, S. Yarlagadda, J.W. Gillespie, Accelerated curing of adhesives in bonded joints by induction heating, J. Compos. Mater. 33 (1999) 1643–1664 ⟨http://cat.inist.fr/?aModele=afficheN & cpsidt=1961962⟩ (accessed 19.05.16).
[11] S. Ye, N.B. Cramer, B.E. Stevens, R.L. Sani, C.N. Bowman, Induction Curing of Thiol Â Acrylate and Thiol Â Ene Composite Systems, 2011, pp. 4988 4996.
[12] K.J. Miller, K.N. Collier, H.B. Soll-Morris, R. Swaminathan, M.E. McHenry, Induction heating of FeCo nanoparticles for rapid rf curing of epoxy composites, J. Appl. Phys. 105 (2009) 1–4. http://dx.doi.org/10.1063/1.3073833.
[13] R.E. Rosensweig, Heating magnetic fluid with alternating magnetic field, J. Magn. Magn. Mater. 252 (2002) 370–374. http://dx.doi.org/10.1016/S0304-8853(02)00706-0.
[14] G. Glöckl, R. Hergt, M. Zeisberger, The effect of field parameters, nanoparticle properties and immobilization on the specific heating power in magnetic particle hyperthermia, J. Phys: Condens. Matter 18 (2006) S2935–S2949. http://dx.doi.org/10.1088/0953-8984/18/38/S27.
[15] E.Stoner, E.Wohlfarth, A mechanism of magnetic hysteresis in heterogeneous alloys, ... London. Ser. A. Math. Phys. .... 240559–642. ⟨http://www.jstor.org/stable/10.2307/91421⟩ (accessed 23.10.13), 1948.
[16] N. a. Usov, Low frequency hysteresis loops of superparamagnetic nanoparticles with uniaxial anisotropy, J. Appl. Phys. 107 (2010) 123909. http://dx.doi.org/10.1063/1.3445879.
[17] N. a. Usov, Y.B. Grebenshchikov, Hysteresis loops of an assembly of superparamagnetic nanoparticles with uniaxial anisotropy, J. Appl. Phys. 106 (2009) 23917. http://dx.doi.org/10.1063/1.3173280.
[18] D. Serantes, D. Baldomir, C. Martinez-Boubeta, K. Simeonidis, M. Angelakeris, E. Natividad, M. Castro, A. Mediano, D.-X. Chen, A. Sanchez, L. Balcells, B. Martinez, Influence of dipolar interactions on hyperthermia properties of ferromagnetic particles, J. Appl. Phys. 108 (2010) 73918. http://dx.doi.org/10.1063/1.3488881.
[19] L.-M. Lacroix, R.B. Malaki, J. Carrey, S. Lachaize, M. Respaud, G.F. Goya, B. Chaudret, Magnetic hyperthermia in single-domain monodisperse FeCo nanoparticles: evidences for Stoner-Wohlfarth behavior and large losses, J. Appl. Phys. 105 (2009) 23911. http://dx.doi.org/10.1063/1.3068195.
[20] G. Vallejo-Fernandez, O. Whear, a.G. Roca, S. Hussain, J. Timmis, V. Patel, K. O'Grady, Mechanisms of hyperthermia in magnetic nanoparticles, J. Phys. D: Appl. Phys. 46 (2013) 312001. http://dx.doi.org/10.1088/0022-3727/46/31/312001.
[21] C. Rümenapp, F.E. Wagner, B. Gleich, Monitoring of the aging of magnetic nanoparticles using Mössbauer spectroscopy, J. Magn. Magn. Mater. 380 (2015) 241–245. http://dx.doi.org/10.1016/j.jmmm.2014.09.071.
[22] E. Lima Jr, E. De Biasi, Heat generation in agglomerated ferrite nanoparticles in an alternating magnetic field, J. Phys. D: Appl. Phys. 46 (2013) 45002. http://dx.doi.org/10.1088/0022-3727/46/4/045002.